Published in final edited form as:
Mol Cancer Res. 2012 December ; 10(12): 1567–1579. doi:10.1158/1541-7786.MCR-12-0209-T.

The Role of Bcl-xL in Synergistic Induction of Apoptosis by Mapatumumab and Oxaliplatin in Combination with Hyperthermia on Human Colon Cancer

Xinxin Song[1], **Seog-Young Kim**[1], and **Yong J. Lee**[1,2]

[1]Department of Surgery, School of Medicine, University of Pittsburgh, Pittsburgh, Pennsylvania 15213, USA

[2]Department of Pharmacology & Chemical Biology, School of Medicine, University of Pittsburgh, Pittsburgh, Pennsylvania 15213, USA

Abstract

Colorectal cancer is the third leading cause of cancer-related mortality in the world. The main cause of death of colorectal cancer is hepatic metastases which can be treated using isolated hepatic perfusion (IHP), allowing treatment of colorectal metastasis with various methods. In this study we present a novel potent multimodality strategy comprising humanized death receptor 4 (DR4) antibody mapatumumab (Mapa) in combination with oxaliplatin and hyperthermia to treat human colon cancer cells. Oxaliplatin and hyperthermia sensitized colon cancer cells to Mapa in the mitochondrial dependent apoptotic pathway and increased reactive oxygen species production, leading to Bcl-xL phosphorylation at Serine 62 in a c-Jun N-terminal kinase (JNK)-dependent manner. Overexpression of Bcl-xL reduced the efficacy of the multimodality treatment, while phosphorylation of Bcl-xL decreased its anti-apoptotic activity. The multimodality treatment dissociated Bcl-xL from Bax, allowing Bax oligomerization to induce cytochrome *c* release from mitochondria. In addition, the multimodality treatment significantly inhibited colorectal cancer xenografts' tumor growth. The successful outcome of this study will support the application of multimodality strategy to colorectal hepatic metastases.

Keywords

Mapatumumab; Hyperthermia; Oxaliplatin; Mitochondria-dependent pathway

INTRODUCTION

Molecular targeted therapies such as antibodies and small molecule inhibitors have emerged as an important breakthrough in human cancer therapeutics. One such agent, tumor necrosis factor (TNF)-related apoptosis-inducing ligand (TRAIL), is believed to selectively induce apoptosis, but controversy regarding the use of TRAIL has centered on its potential hepatotoxicity especially when combined with other drugs (1). This potential problem may be circumvented by the use of specific humanized anti-TRAIL receptor monoclonal antibodies (1). Such agnostic antibodies can induce cell death while avoiding decoy-

All correspondence should be addressed to Dr. Yong J. Lee, Department of Surgery, University of Pittsburgh, Hillman Cancer Center, 5117 Centre Ave. Room 1.46C, Pittsburgh, PA 15213, U.S.A., Tel (412) 623-3268, Fax (412) 623-7709, leeyj@upmc.edu..

Contributions: S. X. performed research and wrote the paper; K. S. performed research; L.Y. designed the research and revised and approved the paper.

Conflict-of-interest disclosure: The authors declare no competing financial interests.

receptor-mediated neutralization of the signal. Moreover, the agonistic antibody may also activate Fc-mediated antibody effector functions such as antibody-dependent cellular cytotoxicity and complement-mediated cytotoxicity (2). In this study, we employed the DR4 agonistic antibody mapatumumab (Mapa) as one of options for the treatment of colon cancer.

Mapa is a fully human IgG1 agonistic monoclonal antibody which exclusively targets and activates DR4 with very high specificity and affinity. Apoptosis-inducing mechanisms of Mapa are thought to be similar to apoptosis mediated by TRAIL (3). TRAIL-induced cell death is triggered by the interaction of the ligand with receptors to assemble the death-inducing signaling complex. This complex triggers association of the intracellular adaptor, Fas-associated death domain (FADD). FADD then recruits procaspase-8, which undergoes spontaneous autoactivation. Following the extrinsic pathway, activated caspase-8 activates the effector caspases-3, -6 and -7 which cleave cellular substrates to execute cell death (4). Previous data suggest the existence of cross-talk between the extrinsic and intrinsic death signaling pathways. Caspase-8, which can proteolytically activate the BH3 only family member Bid, induces Baxand Bak-mediated release of cytochrome *c* and Smac/DIABLO from mitochondria and triggers intrinsic apoptosis (5). However, substantial numbers of cancer cells are resistant to Mapa. This resistance can occur at different points in the signaling pathways, such as dysfunctions of the death receptors DR4 and DR5, defects in FADD, overexpression of anti-apoptotic proteins, loss of pro-apoptotic proteins, etc (6). It is therefore critical to develop applicable strategies to overcome this resistance.

We previously reported that hyperthermia (41–42°C) has a synergistic effect with Mapa in causing cytotoxicity in CX-1 human colorectal cancer through the mitochondria-dependent pathway (7). Hyperthermia, a treatment often used with isolated hepatic perfusion (IHP), maximizes the tumor damage while preserving the surrounding normal tissue. In this study, we developed a multimodality treatment using Mapa concurrently with hyperthermia and oxaliplatin to treat human colon cancer. Oxaliplatin, a common chemotherapeutic agent for colon cancer, is thought to trigger cell death mainly by inducing platinum-DNA adduct (8). We report here that the multimodality treatment of Mapa concurrent with oxaliplatin and hyperthermia induces BclxL phosphorylation at the serine 62 (S62) residue in a JNK-dependent manner and leads to the oligomerization of Bax. This then allows the release of cytochrome *c* from the mitochondria and induces a synergistic effect *in vitro* and *in vivo*.

MATERIALS AND METHODS

Cell cultures

Human colorectal carcinoma CX-1 cells, which were obtained from Dr. J.M. Jessup (NIH), were cultured in RPMI-1640 medium (Gibco BRL) containing 10% fetal bovine serum (HyClone). The human colorectal carcinoma HCT116 Bax-containing ($Bax^{+/+}$), Bax-deficient ($Bax^{-/-}$), Puma-containing ($Puma^{+/+}$) and Puma-deficient ($Puma^{-/-}$) cell lines kindly provided by Dr. B. Vogelstein (Johns Hopkins University) were cultured in McCoy's 5A medium (Gibco-BRL) containing 10% fetal bovine serum. Mycoplasma test was performed routinely for all cell lines.

Reagents and antibodies

Oxaliplatin, N-acetylcysteine (NAC), apogossypol hexaacetate, hygromycin and protease inhibitor cocktail were obtained from Sigma Chemical Co. Mapa was from Human Genome Sciences. JNK inhibitor (SP600125) and G418 were from Calbiochem. Rabbit polyclonal anti-phosphorylated JNK, anti-caspase-8, anti-Bax, anti-Puma, anti-COX-IV, anti-Bcl-xL, and anti-HA antibody were from Cell Signaling. Anti-p-Bcl-xL (S62) antibody was from

Chemicon/Millipore and Abcam. Anti-nucleolin antibody was from Abcam. Anti-JNK and anticaspase-3 antibodies were from Santa Cruz. Anti-caspase-9 antibody was from Upstate Biotechnology. Monoclonal antibodies included anti-PARP antibody from Biomol Research Laboratory, anti-cytochrome *c* antibody from PharMingen and anti-actin antibody from ICN.

Treatment

Cells were pretreated with oxaliplatin and exposed to hyperthermia in the presence/absence of Mapa and oxaliplatin. For hyperthermia, cells were sealed with parafilm and placed in a circulating water bath (Thomas Scientific), which was maintained within 0.02°C of the desired temperature.

Survival assay

For trypan blue exclusion assay, trypsinized cells were pelleted and resuspended in 0.2 ml of medium, 0.5 ml of 0.4% trypan blue solution, and 0.3 ml of phosphate-buffered saline solution (PBS) and incubated at room temperature for 15 min. At least 300 cells were counted under a light microscope for each survival determination. For colony formation assay, after treatment, cells were trypsinized, counted and plated at appropriate dilutions (200 - 1×10^6 cells/dish). The dishes were incubated at 37°C for 7–14 days to allow colony formation. Colonies were fixed by 0.5% crystal violet solution and counted. For every surviving fraction, the plating efficiency value was normalized.

Cell proliferation assay

For cell proliferation assay, 4×10^5 cells were plated into 60-mm Petri dish. Cells were treated and counted various times after treatment and then results were plotted on a graph.

Annexin V binding

Cells were harvested and stained with anti-human Annexin V antibody and PI. The immunostaining was terminated by addition of binding buffer and cells were immediately analyzed by flow cytometry.

Cell cycle analysis

Cells were harvested and fixed with 70% ethanol. Cells were stained with PI/RNase staining buffer (BD Pharmingen) for 15 min at room temperature and analyzed by flow cytometry.

Measurement of reactive oxygen species (ROS) generation

The cells were stained with 20 mM 2',7'-dichlorofluorescein diacetate (DCFH-DA) (Molecular Probes) for 30 min at 37°C, and the fluorescence was detected by a fluorescence microscope.

Stable transfection

Cells stably overexpressing HA-Bcl-xL wild-type (WT) or mutant types were prepared by transfecting CX-1 cells with human Bcl-xL tagged with HA epitope in pCDNA3.1 vector: HA-Bcl-xL-WT, HA-Bcl-xL-S62A (Ser62Ala) and HA-Bcl-xL-S62D (Ser62Asp) (a kind gift from Dr. Timothy C. Chambers) and maintained in 500 μg/ml G418. pSilencer-Bcl-xL or pSilencer control was transfected into CX-1 cells, and hygromycin B (250 μg/ml)-resistant cell clones were isolated.

Immunoprecipitation

Briefly, cells were lysed in CHAPS lysis buffer with protease inhibitor cocktail (Calbiochem). Cell lysates were clarified by centrifugation at 13,000 rpm for 15 min, and protein concentration was determined by BCA Protein Assay Reagent (Pierce). For immunoprecipitation, 0.5–1 mg of lysate was incubated with 1.5 μg of rabbit anti-Bax or anti- HA antibody or rabbit IgG (Santa Cruz) at 4°C overnight, followed by the addition of protein A-agarose beads (Santa Cruz) and rotation at room temperature for 2 h. The beads were washed and resuspended in sodium dodecyl sulfate (SDS) sample buffer and followed by immunoblot analysis.

Confocal microscope

HCT116 $Bax^{-/-}$ cells were transfected with Lipofectamine 2000 (Invitrogen) with plasmids containing green fluorescent protein fused to Bax (pBax-GFP) and/or red fluorescent protein fused to Bcl-xL (pBcl-xL-RFP) (a kind gift from Dr. Justin Cross and Dr. Ingram Iaccarino). Twenty four hours after transfection, cells were treated with oxaliplatin/Mapa/hyperthermia as described above. Mitochondria were stained with MitoTracker (Invitrogen). Cellular DNA was stained with DRAQ5 (Cell Signaling). Phosphorylated Bcl-xL was stained with anti-p-Bcl-xL antibody. HA-Bcl-xL-WT, HA-Bcl-xL-S62A and HA-Bcl-xL-S62D were stained with anti-HA antibody. Nucleolin was stained with anti-nucleolin antibody. Slides were visualized using an inverted Leica TCSSL laser scanning confocal microscope. For digital image analysis, the software Adobe Photoshop 7.0 version was used.

Bax oligomerization

Cells were pelleted and resuspended in HB buffer. The cell suspension was homogenized, and spun at 1,000×g for 15 min at 4°C. The supernatant was transferred and spun at 10,000×g for 15 min at 4°C to pellet mitochondria. Aliquots of isolated mitochondrial fractions and cytosolic fractions were cross-linked with 1 mM dithiobis (Pierce). Samples were subjected to SDS-PAGE under non-denaturing conditions followed by immunoblotting for Bax.

JC-1 mitochondrial membrane potential assay

Cells were stained using JC-1 mitochondrial membrane potential detection kit (Cayman) and analyzed by flow cytometry. Fluorescence intensity was measured with the Accuri C6 Flow Cytometer (Accuri Cytometers). Results were analyzed with VenturiOne software (Applied Cytometry).

Immunoblot analysis

Cells were lysed with 1×Laemmli lysis buffer and boiled for 10 min. Protein content was measured with BCA Protein Assay Reagent (Pierce). Proteins were separated by SDS-PAGE and electrophoretically transferred to nitrocellulose membrane which was blocked for 1 h. The membrane was incubated with primary antibody at room temperature for 1.5 h. Horseradish peroxidase conjugated IgG was used as the secondary antibody. Immunoreactive protein was visualized by the chemiluminescence protocol (Amersham).

Animal model

Human colon adenocarcinoma CX-1 tumors were established by subcutaneously injecting 10^6 cells into the right hind leg of 6–8 week old male NU/NU mice (Charles River Labs). Prior to treatment with oxaliplatin/Mapa/hyperthermia, tumor size was measured 2–3 times per week until the volume reached above 200 mm^3. Tumor volume was calculated as $W^2 \times L \times 0.52$ where L is the largest diameter and W is the diameter perpendicular to L. After establishment of these tumor xenografts, mice were randomized into eight groups of five

mice per group. Oxaliplatin was administered by intraperitoneal injection. One hour later, Mapa was administrated by intratumoral injection and then tumor bearing legs were immersed in a water bath at 42°C for 1 h. All procedures involving the mice were in accordance with the Guide for the Care and Use of Laboratory Animals and on a protocol approved by the Institutional Animal Care and Use Committee of the University of Pittsburgh.

TUNEL assay

The terminal deoxynucleotidyl transferase-mediated dUTP-biotin nick end labeling (TUNEL) method was performed after the protocol of TACS 2 TdT-Fluor In Situ Apoptosis Detection Kit (Trevigen, Gaithersburg, MD). Briefly, sections of formalin-fixed, paraffin-embedded tissues were deparaffinized, then washed with PBS and permeabilized with Proteinase K. DNA strand breaks were then end-labeled with terminal transferase, and the labeled DNA was visualized by fluorescence microscopy (magnification ×200).

Statistical analysis

Statistical analysis was carried out using Graphpad InStat 3 software (GraphPad Software). Results were considered statistically significant at $P<0.05$.

RESULTS

Effect of oxaliplatin and hyperthermia on Mapa-induced cytotoxicity in CX-1 cells

To investigate the efficacy of oxaliplatin/Mapa/hyperthermia, cells were incubated with oxaliplatin for 20 h and exposed to normothermic or hyperthermic conditions for 1 h in the presence/absence of Mapa and oxaliplatin, and then incubated for 3 h at 37°C in the presence/absence of Mapa and oxaliplatin. As the doses of Mapa or oxaliplatin increased, the cell surface began blebbing and apoptotic bodies were formed. In particular, there was a dramatic increase in the number of rounded cells and detached cells during the modality treatment oxaliplatin/Mapa/hyperthermia (Fig. 1A). Similar results were obtained for survival measured by the trypan blue exclusion assay which was performed immediately after treatment and indicates physiological death (Fig. 1B). Synergistic interactions between oxaliplatin/Mapa/hyperthermia were also observed by colony formation assay which took 1–2 weeks after treatment and indicates reproductive death (Fig. 1C). Cell proliferation assay was conducted to detect long-term growth in each treatment. The multimodality treatment effectively inhibits cell proliferation (Fig. 1D). Collectively, Mapa, oxaliplatin and hyperthermia induced synergistic cytotoxicity in a dose-dependent manner.

Effect of oxaliplatin and hyperthermia on Mapa-induced apoptosis in CX-1 cells

To clarify whether the cytotoxicity of the multimodality treatment of oxaliplatin/Mapa/hyperthermia is associated with apoptosis, we employed the Annexin V assay (Fig. 2A) and observed that a dramatic synergistic effect was achieved during the multimodality treatment of oxaliplatin/Mapa/hyperthermia. Next, we examined whether the multimodality treatment promotes caspase pathways. Data from Fig. 2B show that treatment with Mapa resulted in activation of caspase 8 and caspase 3, but not caspase 9. Interestingly, hyperthermia in combination with Mapa enhanced Mapa-induced activation of caspases 8 and 3 and activated caspase 9. Treatment with oxaliplatin activated only caspase 9 and 3. Combined Mapa and oxaliplatin treatment enhanced the activation of caspases 8, 9 and 3. Furthermore, a dramatic synergistic activation of caspases 8, 9 and 3 was observed during the multimodality treatment of oxaliplatin/Mapa/hyperthermia. These synergistic effects were also confirmed by determining the hallmark of apoptosis, PARP cleavage (Fig. 2B).

ROS-induced JNK activation in the multimodality treatment

Next, we attempted to investigate the mechanisms by which the multimodality treatment induced apoptosis. Fig. 3A shows that there were significant fluorescence signals of ROS when Mapa was combined with hyperthermia or oxaliplatin. Of note, maximum signals were detected in the multimodality treatment. We also observed that an antioxidant N-acetylcysteine (NAC) pretreatment significantly decreased the signals of ROS. Fig. 3B demonstrates oxaliplatin increased the JNK activation in a dose-dependent manner, and maximum synergistic activation was detected in oxaliplatin/Mapa/hyperthermia. We also observed that pretreatment with NAC significantly blocked the activation of JNK and suppressed the effect of oxaliplatin/Mapa/hyperthermia-induced PARP cleavage (Fig. 3C).

Role of Bcl-xL in the multimodality treatment-induced apoptosis

Bcl-xL is a key anti-apoptotic protein that characteristically undergoes phosphorylation in response to treatment with apoptotic agents (9). In this study, we assessed the status of phosphorylation of Bcl-xL at Ser-62 during multimodality treatment (Fig. 3D). No detectable amounts of phospho-Bcl-xL were observed in the control or single treatment. Phosphorylated Bcl-xL was detected during treatment with oxaliplatin and Mapa. Interestingly, a large amount of phospho-Bcl-xL was detected in the multimodality treatment of oxaliplatin/Mapa/hyperthermia. Pretreatment with SP600125 significantly reduced oxaliplatin/Mapa/hyperthermia-induced PARP cleavage in CX-1 cells, indicating that the JNK pathway was crucial for multimodality treatment-induced apoptosis (Fig. 3E). Noticeably, SP600125 highly reduced the level of Bcl-xL phosphorylation in CX-1 cells, which provides strong evidence that multimodality treatment-induced Bcl-xL phosphorylation requires JNK activation.

To evaluate the effect of Bcl-xL phosphorylation at Ser 62 on its own anti-apoptotic activity, we established CX-1-derived cell lines stably overexpressing wild-type Bcl-xL (Bcl-xL-WT), Ser62/Ala phospho-defective Bcl-xL mutant (Bcl-xL-S62A), Ser62/Asp phospho-mimic Bcl-xL mutant (Bcl-xL-S62D), or the corresponding empty vector (pcDNA) (Fig. 3F). As expected, overexpression of Bcl-xL-WT prevented oxaliplatin/Mapa/hyperthermia-induced PARP cleavage. Interestingly, overexpression of Bcl-xL-S62D enhanced PARP cleavage, whereas that of Bcl-xL-S62A inhibited PARP cleavage. These data suggest that the level of Bcl-xL and its phosphorylation at S62 play an important role in the multimodality-induced apoptosis.

Multimodality treatment-induced Bcl-xL phosphorylation (Ser62), cell cycle arrest, and translocation of Bcl-xL

It is reported that phosphorylation of the serine-62 residue on Bcl-xL is detected after treatment with microtubule inhibitors or other compounds and its phosphorylation induces G_2/mitotic arrest (9, 10). In this study, we examined whether multimodality treatment induces phosphorylation of Bcl-xL and affects the cell cycle distribution. Data from the kinetics of BclxL phosphorylation show that phosphorylation of Bcl-xL was detected during pretreatment with oxaliplatin as well as treatment with oxaliplatin/Mapa/hyperthermia (Fig. 4A). Interestingly, G_2/M cell-cycle arrest was observed during pretreatment with oxaliplatin and an increase in G_2/M arrest occurred during the multimodality treatment (Fig. 4B). Recent studies have shown that G_2/M arrest is associated with accumulation of a pool of phosphorylated Bcl-xL in nucleolar structures (10). This possibility was investigated by using confocal immunofluorescence microscopy which was undertaken to monitor the location of phospho-Bcl-xL (S62). Control panel in Figure 4C shows residual amounts of phosphorylated Bcl-xL (S62) in untreated cells. The level of phosphorylated Bcl-xL (S62) increased and a pool of phosphorylated Bcl-xL (S62) translocalized from the cytoplasm to the nuclei and nucleoli after oxaliplatin/Mapa/hyperthermia treatment (Fig. 4C). To examine

whether phosphorylation of the S62 residue on Bcl-xL is important for translocation of Bcl-xL, CX-1 cells were stably transfected with HA-Bcl-xL-WT, phospho-defective HA-Bcl-xL-S62A, or phospho-mimic HA-Bcl-xL-S62D. Figure 4D shows that HA-Bcl-xL-WT and HA-Bcl-xL-S62D, but not HA-Bcl-xL-S62A, translocated to the nuclei and nucleoli after oxaliplatin/Mapa/hyperthermia treatment. These results suggest that phosphorylation of Bcl-xL at S62 plays an important role in the translocation of Bcl-xL.

The dissociation of Bcl-xL from Bax in the treatment of Mapa, oxaliplatin and hyperthermia

We next tested whether the multimodality treatments alter the interactions between Bcl-xL and Bax. An interaction between Bcl-xL and Bax was detected by immunoprecipitation assay in control and Mapa-treated cells (Fig. 5A). This interaction was slightly reduced after hyperthermia or oxaliplatin treatment. Notably, Bax was dissociated from Bcl-xL during treatment with oxaliplatin in combination with Mapa or the multimodality treatment oxaliplatin/Mapa/hyperthermia (Fig. 5A). To further study the role of Bcl-xL phosphorylation at S62 on the interaction between Bax and Bcl-xL in response to oxaliplatin/Mapa/hyperthermia treatment, immunoprecipitation assay was performed on Bcl-xL-WT, Bcl-xL-S62A, or Bcl-xLS62D transfected cells. Figure 5B shows that the weakest interaction between Bcl-xL and Bax occurred in untreated Bcl-xL-S62D transfected cells, while dissociation of Bax from Bcl-xL was reduced in Bcl-xL-S62A transfected cells during the multimodality treatment. These observations suggest that phosphorylation of Bcl-xL at S62 plays an important role in BclxL/Bax interaction.

Furthermore, confocal immunfluorescence microscopy assay (Fig. 5C) shows overlapping signals (yellow color) of Bcl-xL-RFP and Bax-GFP. Of note, we observed a large amount of Bcl-xL dissociated from Bax in oxaliplatin/Mapa and oxaliplatin/Mapa/hyperthermia treatment. Previous studies have shown that gossypol, the levorotatory isomer of a natural product isolated from cottonseeds and roots, binds to the BH3 binding groove of Bcl-xL and Bcl-2 and subsequently inhibits the heterodimerization of Bcl-xL or Bcl-2 with proapoptotic proteins such as Bax or Bad (11). In this study, pretreatment with apogossypol hexaacetate sensitized the apoptotic effect of Mapa, oxaliplatin and hyperthermia (Fig. 5D). Moreover, the multimodality treatment-induced apoptosis was markedly enhanced by knockdown of Bcl-xL expression (Fig. 5E). These results suggest that dissociation of Bax from Bcl-xL enhances apoptosis.

Bax oligomerization, localization to the mitochondria and subsequent cytochrome *c* release in the treatment of oxaliplatin, Mapa and hyperthermia

To examine the involvement of Bax in multimodality treatment-induced apoptosis, we employed human colon carcinoma parental HCT116 wild-type (HCT116 WT) and HCT116 $Bax^{-/-}$ cells. As shown in Figures 6A and 6B, HCT116 $Bax^{-/-}$ cells were resistant to PARP cleavage in the multimodality treatment compared to HCT116 WT cells, which clearly indicates that the synergy of oxaliplatin/Mapa/hyperthermia-associated apoptosis is mediated through Bax. Another important protein is the p53 upregulated modulator of apoptosis (PUMA). It is also a pro-apoptotic Bcl-2 protein and is involved in p53-dependent and -independent apoptosis induced by a variety of signals (12). In contrast to HCT116 $Bax^{-/-}$ cells, PUMA-deficient cells were not resistant to PARP cleavage in the multimodality treatment oxaliplatin/Mapa/hyperthermia compared to HCT116 WT cells (Figs. 6A and 6B). These results clearly suggest that PUMA is not involved in oxaliplatin/Mapa/hyperthermia-induced apoptotic death.

Since Bax oligomerization plays an important role in apoptosis, we examined how the multimodality treatment affected Bax oligomerization (Fig. 6C). There was more multimeric Bax oligomerization in the treatment of oxaliplatin/Mapa/hyperthermia compared with the

other treatments. We also observed in confocal assay that more Bax-GFP translocalized to the mitochondria in the multimodality treatment compared to the other treatments (Fig. 6D). As shown in Fig. 6E, cells with intact mitochondrial membrane potential were detected in the upper right quadrant of the plots and those with impaired mitochondrial membrane potential were detected in the lower right quadrant of the plots. A shift to the lower right part of the quadrants (a loss of membrane potential) occurred in the multimodality treatment oxaliplatin/Mapa/hyperthermia. More importantly, Fig. 6F shows that more cytochrome *c* release occurred during multimodality treatment oxaliplatin/Mapa/hyperthermia.

Effect of oxaliplatin, Mapa and hyperthermia on the growth of CX-1 xenograft tumors

Finally, *in vivo* studies were performed to examine the effect of the multimodality treatment oxaliplatin/Mapa/hyperthermia on growth of xenograft tumors. Figure 7 shows that hyperthermia alone has no effect on tumor growth compared with the control group. The effect of oxaliplatin alone on tumor growth was observed 6 days after treatment compared to the control group; however, there was only a slight, not statistically significant difference 12 days after treatment (Fig. 7B). Mapa alone caused a statistically significantly decrease of tumor growth ($P<0.05$). Moreover, bitherapy of Mapa combined with hyperthermia or Mapa combined with oxaliplatin caused a significant decrease of CX-1 tumor growth compared with single treatment groups ($P<0.01$). In particular, the multimodality treatment was significantly more effective at inhibiting xenograft tumor growth than the single treatments or any other bitherapy strategies. TUNEL assay confirmed many apoptotic deaths in xenograft tumor tissue at day 12 after oxaliplatin/Mapa/hyperthermia treatment in comparison to sham group (Fig.7C).

DISCUSSION

Previous phase II trials showed that no/little clinical activity of single-agent Mapa was observed in patients with advanced refractory colorectal cancer or non-small cell lung cancer (13). So enhancing the effect of Mapa is required for clinical application of Mapa. Various chemotherapeutic agents such as oxaliplatin, cisplatin, 5-FU, and paclitaxel have been shown to enhance and sensitize the apoptosis-inducing capacity of targeted therapies (14). Most of the research focused on chemotherapeutic agents to increase the effect of TRAIL-based therapy in a xenograft model system (15). To the best of our knowledge, we are the first to test the efficacy of combined Mapa + oxaliplatin + hyperthermia in colon cancer cells and mouse xenograft tumor model, suggesting that this multimodality approach will be applicable to improve the clinical efficacy of Mapa for treatment of colon cancer.

Hyperthermia has been explored as an anticancer agent for many decades. While the treatment effects of hyperthermia as a single agent are limited, its ability to potentiate the effects of standard chemotherapies has generated lasting interest (16). Our laboratory has focused on identifying strategies for thermal sensitization in an attempt to improve the clinical efficacy of IHP. We previously reported that hyperthermia combined with TRAIL induces cytotoxicity by facilitating activation of caspases through mitochondria-dependent cytochrome *c* release in colorectal cancer cells (7). In this study, we observed that hyperthermia in combination with Mapa and oxaliplatin elevates the intracellular level of ROS and activates the JNK-Bcl-xL-Bax signal transduction pathway. Data from the kinetics of Bcl-xL phosphorylation indicates that Bcl-xL phosphorylation is an early event and p-Bcl-xL-Bax dissociation is a cause of cell death through cytochrome *c* release (Figs. 3E, 3F, 4A, and 6). Several researchers have revealed that hyperthermia induces an increase in ROS and increased antioxidant enzyme levels result in protection of cells from oxidative stress (17). It is well known that ROS is generated through several intracellular sources including mitochondrial electron transport chain and peroxisomal cytochrome P-450 oxidases as well as endogenous enzyme systems (18). Previous studies suggest that disruption of the

mitochondria electron transport chain is the main source of ROS generation during hyperthermia (17). Our data and literatures (19) show that oxaliplatin/TRAIL treatment elevates the intracellular level o f R O S. Hyperthermia in combination with oxaliplatin/Mapa may facilitate the disruption of the mitochondrial electron transport chain and increase ROS generation. We previously observed that ROS can be sensed through thioredoxin (TRX) and glutaredoxin (GRX), resulting in activation of the ASK1 (apoptosis signal-regulating kinase 1)-MEK (mitogen extracellular kinase)-MAPK (mitogen-activated protein kinase) signal transduction pathway (20). These sensor molecules may be converted to the intramolecular disulfide form of TRX-(S-S) and GRX-(S-S) during treatment of oxaliplatin/Mapa/hyperthermia. This oxidized form of TRX and GRX may dissociate from ASK1 and consequently activate the ASK1-MEK-JNK-Bcl-xL-Bax signal transduction pathway (21).

Bcl-xL, a key antiapoptotic molecule, is a target for JNK signaling. Bcl-xL undergoes phosphorylation in response to microtubule inhibitors and other apoptotic stimuli including ionizing radiation or chemotherapy (9). Our study for the first time revealed that hyperthermia and oxaliplatin synergistically promoted Bcl-xL phosphorylation and thus significantly sensitized Mapa-induced apoptosis. We also observed that Bcl-xL phosphorylation required activated JNK, which can recognize a proline residue on the carboxyl side of the phosphoacceptor (22). Some studies reported phosphorylation to occur on serine 62, while others reported it to occur on threonines 47 and 115 (23, 24). This study with site-directed mutagenesis at Ser-62 showed that cells expressing a validated phospho-defective Bcl-xL mutant are resistant to the multimodality treatment-induced apoptosis, whereas cells expressing a phospho-mimic Bcl-xL are sensitive to the multimodality-induced apoptosis, indicating that phosphorylation at Ser-62 is a key regulatory mechanism for antagonizing anti-apoptotic function in the multimodality treatment.

Phospho-Bcl-xL (Ser62) has been reported to play a key role at DNA damage-induced G_2/M arrest (10). In this study we observed that phosphorylation of Bcl-xL at S62 after oxaliplatin/Mapa/hyperthermia treatment was associated with G_2/M arrest (Fig. 4). This is probably due to translocation of Bcl-xL in the nucleus and nucleolus during the G2 checkpoint (10). Previous studies demonstrate that Bcl-xL's function in cell cycle arrest is distinct from its function in apoptosis (10).

It is reported that Bcl-xL inhibits and maintains Bax in the cytosol by constant retro-translocation of mitochondrial Bax which undergoes a conformational shift under apoptotic signaling, and inserts into the outer mitochondrial membrane (25). We observed in this study that upon Bcl-xL phosphorylation, the interaction of Bax and Bcl-xL was impaired, resulting in Bax translocating to the mitochondria. We also observed that a weak interaction between Bax and phospho-mimic Bcl-xL-S62D and Bcl-xL/Bax interaction was less impaired in Bcl-xL-S62A transfected cells indicating Bcl-xL phosphorylation at S62 plays an important role in Bcl-xL/Bax interaction. Disruption of the interaction of Bcl-xL and proapoptotic proteins by apogossypol hexaacetate or knockdown of Bcl-xL sensitizes the effect of the multimodality treatment, which confirms the involvement of Bcl-xL in the multimodality treatment.

We also observed that that Bax but not PUMA is involved in the synergistic effect of the multimodality treatment in this study. However, data from Figure 6B implies that Bax is necessary but not entirely sufficient since there is still some PARP cleavage in $Bax^{-/-}$ cells which suggest that multimodality treatment-induced apoptosis occurs through the mitochondria-independent pathway as well as the mitochondria-dependent pathway. Obviously, our next step will be to investigate the involvement of the mitochondria-independent pathway in the multimodality treatment-induced apoptosis.

Taken together, our results reveal that treatment of hyperthermia concurrently with a DNA-damaging agent, such as oxaliplatin, can synergize Mapa-induced apoptosis *in vitro* and *in vivo*. Inactivating Bcl-xL represents a good strategy to enhance sensitivity to apoptosis. Given the facts that hyperthermia has a favorable safety profile, oxaliplatin is a commonly used chemotherapeutic drug for colon cancers, and Mapa currently is undergoing clinical testing (26), this multimodality treatment has an excellent translational potential and should be considered for colorectal hepatic metastases treatment in clinics.

Acknowledgments

We thank Dr. Patrick Kaminker from Human Genome Sciences who provided us with mapatumumab, Dr. Justin Cross and Dr. Ingram Iaccarino for providing pBax-GFP and Bcl-xL-RFP, and Dr. Timothy C. Chambers who provided pBcl-xL-WT, pBcl-xL-S62A and pBcl-xLS62D.

This work was supported by the following grants: NCI grant fund (CA140554) and DOD-CDMRP funds (BC103217: W81XWH-11-1-0128). This project used the UPCI Core Facility and was supported in part by award P30CA047904.

Abbreviations used in this paper

DR	death receptor
FADD	Fas-associated death domain
IHP	isolated hepatic perfusion
JNK	c-Jun N-terminal kinase
Mapa	mapatumumab
PARP	poly (ADP-ribose) polymerase
Puma	p53 up-regulated modulator of apoptosis
ROS	reactive oxygen species
S62A	serine 62 alanine
S62D	serine 62 asparagine
TRAIL	TNF-related apoptosis-inducing ligand

References

1. Koschny R, Ganten TM, Sykora J, Haas TL, Sprick MR, Kolb A, et al. TRAIL/bortezomib cotreatment is potentially hepatotoxic but induces cancer-specific apoptosis within a therapeutic window. Hepatology. 2007; 45:649–658. [PubMed: 17326159]
2. Maddipatla S, Hernandez-Ilizaliturri FJ, Knight J, Czuczman MS. Augmented antitumor activity against B-cell lymphoma by a combination of monoclonal antibodies targeting TRAIL-R1 and CD20. Clin Cancer Res. 2007; 13:4556–4564. [PubMed: 17671142]
3. Pukac L, Kanakaraj P, Humphreys R, Alderson R, Bloom M, Sung C, et al. HGS-ETR1, a fully human TRAIL-receptor 1 monoclonal antibody, induces cell death in multiple tumour types in vitro and in vivo. Br J Cancer. 2005; 92:1430–1441. [PubMed: 15846298]
4. Sprick MR, Weigand MA, Rieser E, Rauch CT, Juo P, Blenis J, et al. FADD/MORT1 and caspase-8 are recruited to TRAIL receptors 1 and 2 and are essential for apoptosis mediated by TRAIL receptor 2. Immunity. 2000; 12:599–609. [PubMed: 10894160]
5. Basu A, Castle VP, Bouziane M, Bhalla K, Haldar S. Crosstalk between extrinsic and intrinsic cell death pathways in pancreatic cancer: synergistic action of estrogen metabolite and ligands of death receptor family. Cancer Res. 2006; 66:4309–4318. [PubMed: 16618756]

6. Zhang L, Fang B. Mechanisms of resistance to TRAIL-induced apoptosis in cancer. Cancer Gene Ther. 2005; 12:228–237. [PubMed: 15550937]
7. Song X, Kim HC, Kim SY, Basse P, Park BH, Lee BC, et al. Hyperthermia-enhanced TRAIL- and mapatumumab-induced apoptotic death is mediated through mitochondria in human colon cancer cells. J Cell Biochem. 2011
8. Raymond E, Faivre S, Chaney S, Woynarowski J, Cvitkovic E. Cellular and molecular pharmacology of oxaliplatin. Mol Cancer Ther. 2002; 1:227–235. [PubMed: 12467217]
9. Upreti M, Galitovskaya EN, Chu R, Tackett AJ, Terrano DT, Granell S, et al. Identification of the major phosphorylation site in Bcl-xL induced by microtubule inhibitors and analysis of its functional significance. J Biol Chem. 2008; 283:35517–35525. [PubMed: 18974096]
10. Wang J, Beauchemin M, Bertrand R. Phospho-Bcl-xL(Ser62) plays a key role at DNA damage-induced G 2 checkpoint. Cell Cycle. 2012; 11:2159–2169. [PubMed: 22617334]
11. Zhai D, Jin C, Satterthwait AC, Reed JC. Comparison of chemical inhibitors of antiapoptotic Bcl-2-family proteins. Cell Death Differ. 2006; 13:1419–1421. [PubMed: 16645636]
12. Yu J, Zhang L. PUMA, a potent killer with or without p53. Oncogene. 2008; 27(Suppl 1):S71–S83. [PubMed: 19641508]
13. Trarbach T, Moehler M, Heinemann V, Kohne CH, Przyborek M, Schulz C, et al. Phase II trial of mapatumumab, a fully human agonistic monoclonal antibody that targets and activates the tumour necrosis factor apoptosis-inducing ligand receptor-1 (TRAIL-R1), in patients with refractory colorectal cancer. Br J Cancer. 2010; 102:506–512. [PubMed: 20068564]
14. Belyanskaya LL, Marti TM, Hopkins-Donaldson S, Kurtz S, Felley-Bosco E, Stahel RA. Human agonistic TRAIL receptor antibodies Mapatumumab and Lexatumumab induce apoptosis in malignant mesothelioma and act synergistically with cisplatin. Mol Cancer. 2007; 6:66. [PubMed: 17953743]
15. Fan QL, Zou WY, Song LH, Wei W. Synergistic antitumor activity of TRAIL combined with chemotherapeutic agents in A549 cell lines in vitro and in vivo. Cancer Chemother Pharmacol. 2005; 55:189–196. [PubMed: 15290100]
16. Hegewisch-Becker S, Gruber Y, Corovic A, Pichlmeier U, Atanackovic D, Nierhaus A, et al. Whole-body hyperthermia (41.8 degrees C) combined with bimonthly oxaliplatin, high-dose leucovorin and 5-fluorouracil 48-hour continuous infusion in pretreated metastatic colorectal cancer: a phase II study. Ann Oncol. 2002; 13:1197–1204. [PubMed: 12181242]
17. Venkataraman S, Wagner BA, Jiang X, Wang HP, Schafer FQ, Ritchie JM, et al. Overexpression of manganese superoxide dismutase promotes the survival of prostate cancer cells exposed to hyperthermia. Free Radic Res. 2004; 38:1119–1132. [PubMed: 15512801]
18. Gamaley IA, Klyubin IV. Roles of reactive oxygen species: signaling and regulation of cellular functions. Int Rev Cytol. 1999; 188:203–255. [PubMed: 10208013]
19. Choi K, Ryu SW, Song S, Choi H, Kang SW, Choi C. Caspase-dependent generation of reactive oxygen species in human astrocytoma cells contributes to resistance to TRAIL-mediated apoptosis. Cell Death Differ. 2010; 17:833–845. [PubMed: 19876066]
20. Song JJ, Lee YJ. Differential role of glutaredoxin and thioredoxin in metabolic oxidative stress-induced activation of apoptosis signal-regulating kinase 1. Biochem J. 2003; 373:845–853. [PubMed: 12723971]
21. Song JJ, Lee YJ. Catalase, but not MnSOD, inhibits glucose deprivation-activated ASK1-MEK-MAPK signal transduction pathway and prevents relocalization of Daxx: hydrogen peroxide as a major second messenger of metabolic oxidative stress. J Cell Biochem. 2003; 90:304–314. [PubMed: 14505347]
22. Ubersax JA, Ferrell JE Jr. Mechanisms of specificity in protein phosphorylation. Nat Rev Mol Cell Biol. 2007; 8:530–541. [PubMed: 17585314]
23. Basu A, Haldar S. Identification of a novel Bcl-xL phosphorylation site regulating the sensitivity of taxol- or 2-methoxyestradiol-induced apoptosis. FEBS Lett. 2003; 538:41–47. [PubMed: 12633850]
24. Kharbanda S, Saxena S, Yoshida K, Pandey P, Kaneki M, Wang Q, et al. Translocation of SAPK/JNK to mitochondria and interaction with Bcl-x(L) in response to DNA damage. J Biol Chem. 2000; 275:322–327. [PubMed: 10617621]

25. Edlich F, Banerjee S, Suzuki M, Cleland MM, Arnoult D, Wang C, et al. Bcl-x(L) retrotranslocates Bax from the mitochondria into the cytosol. Cell. 2011; 145:104–116. [PubMed: 21458670]
26. Younes A, Vose JM, Zelenetz AD, Smith MR, Burris HA, Ansell SM, et al. A Phase 1b/2 trial of mapatumumab in patients with relapsed/refractory non-Hodgkin's lymphoma. Br J Cancer. 2010; 103:1783–1787. [PubMed: 21081929]

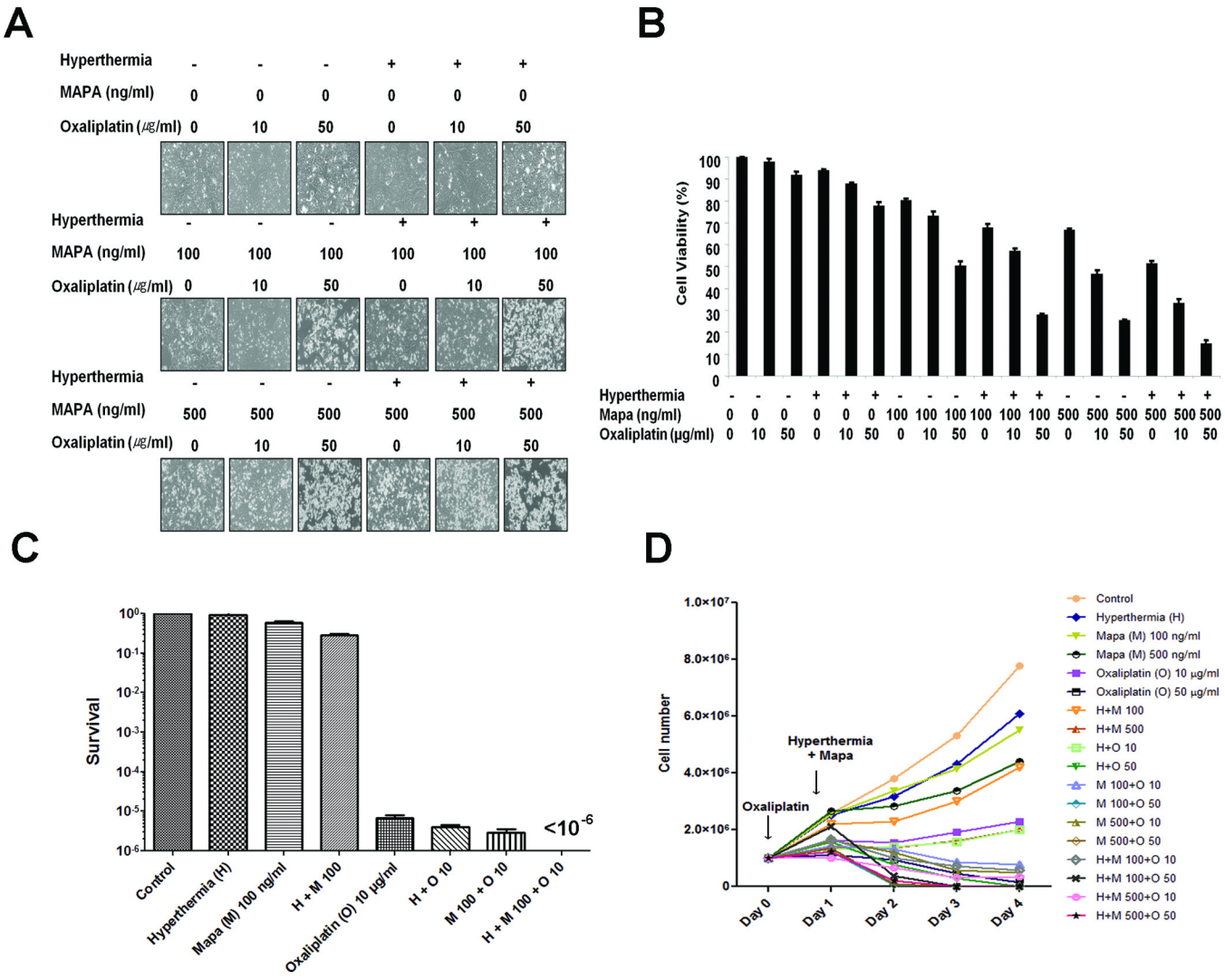

Figure 1. Effect of oxaliplatin and hyperthermia on Mapa-induced cytotoxicity in CX-1 cells

(**A**) CX-1 cells were treated with oxaliplatin for 20 h and exposed to normothermic or hyperthermic (42°C) conditions for 1 h in the presence/absence of Mapa and oxaliplatin and then incubated for 3 h at 37°C in the presence/absence of Mapa and oxaliplatin. Morphological features were analyzed with a phase-contrast microscope. (**B, C**) Survival was analyzed by the trypan blue dye exclusion assay (**B**) or colony formation assay (**C**). Error bars represent SD from triplicate experiments. (**D**) Proliferation assay was performed at day 0–4 after indicated treatment.

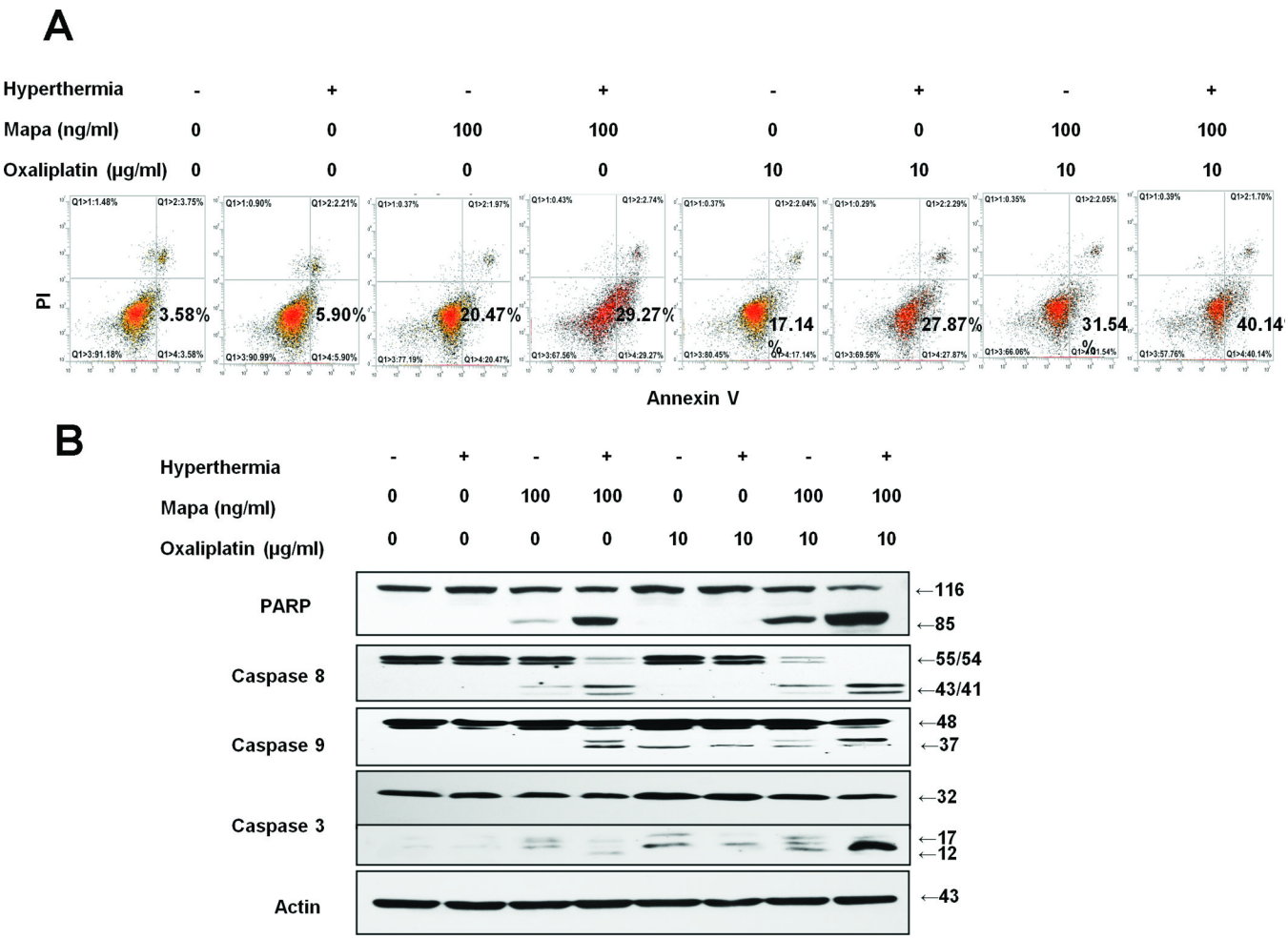

Figure 2. Effect of oxaliplatin and hyperthermia on Mapa-induced apoptosis in CX-1 cells

Cells were treated with oxaliplatin/Mapa/hyperthermia. (**A**) After treatment, cells were stained with fluorescein isothiocyanate (FITC)-Annexin V and propidium iodide (PI). Apoptosis was detected by the flow cytometric assay. (**B**) After treatment, the cleavage of caspase 8, caspase 9, caspase 3, or PARP was detected by immunoblotting. Actin was used to confirm the equal amount of proteins loaded in each lane.

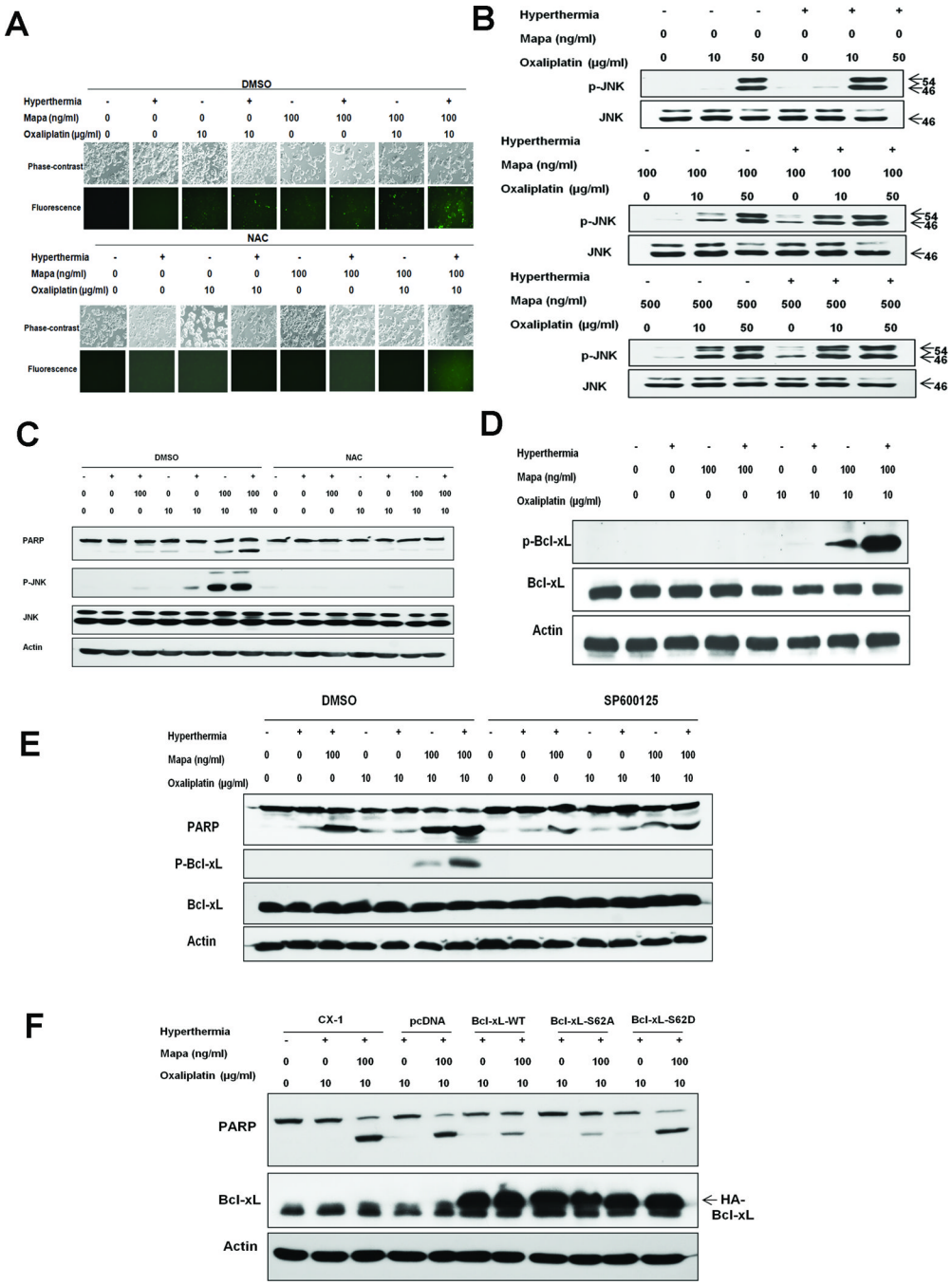

Figure 3. Multimodality treatment-induced ROS production, JNK activation, and Bcl-xL phosphorylation in CX-1 cells

(**A**) Cells were treated with/without 10 mM NAC for 30 min followed by oxaliplatin/Mapa/hyperthermia and incubated with CMH2DCFDA (25 μM). Morphological features and fluorescent signals were detected with a phase-contrast microscope and a fluorescence microscope, respectively. (**B**) Cells were treated with oxaliplatin/Mapa/hyperthermia and immunoblotted with anti-phospho-JNK or anti-JNK antibodies. (**C**) Cells were pretreated with 10 mM NAC for 30 min followed by oxaliplatin/Mapa/hyperthermia. PARP cleavage, phospho-JNK and JNK were detected. (**D**) Cells were treated with oxaliplatin/Mapa/hyperthermia and immunoblotted with anti-phospho-Bcl-xL or anti-Bcl-xL antibody. (**E**)

Cells were pretreated with JNK-1 inhibitor SP600125 followed by oxaliplatin/Mapa/hyperthermia and immunoblotted with anti-PARP, anti-phospho-Bcl-xL and anti-Bcl-xL antibody. (**F**) Transfectants with control plasmid (pcDNA), wild-type Bcl-xL (Bcl-xL-WT), Ser62/Ala phospho-defective Bcl-xL mutant (Bcl-xL-S62A), or Ser62/Asp phospho-mimic Bcl-xL mutant (Bcl-xL-S62D) were treated with oxaliplatin/Mapa/hyperthermia and immunoblotted with anti-PARP or anti-Bcl-xL antibody. Actin was used to confirm the equal amount of proteins loaded in each lane.

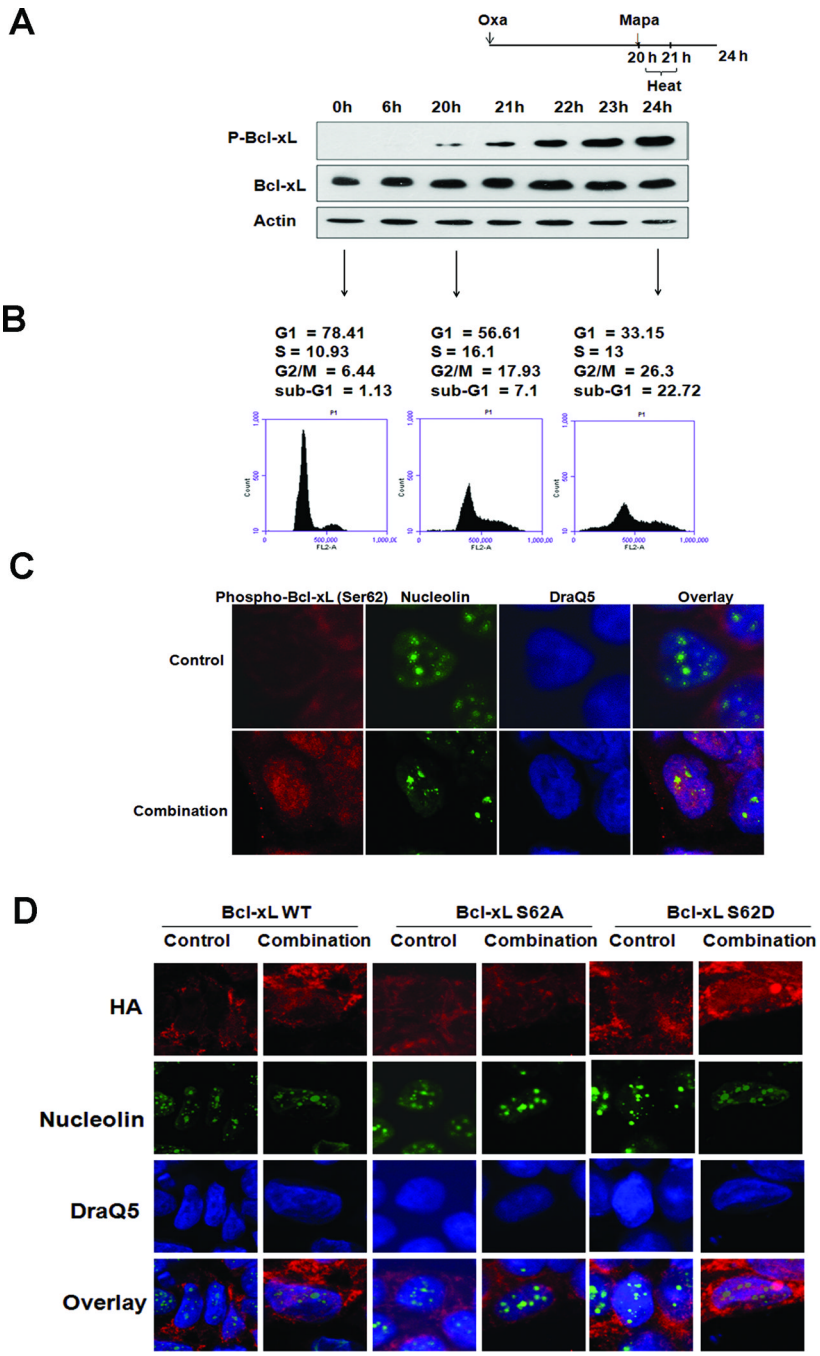

Figure 4. Multimodality treatment-induced Bcl-xL phosphorylation, cell cycle arrest, and translocalization of Bcl-xL

(**A**) Kinetics of Bcl-xL phosphorylation were assessed during treatment with oxaliplatin/Mapa/hyperthermia. **B** Effects of oxaliplatin/Mapa/hyperthermia on cell cycle were determined. (**C, D**) The location of p-Bcl-xL (**C**) and HA-Bcl-xL-WT, HA-Bcl-xL-S62A, and HA-Bcl-xL-S62D (**D**) was examined during oxaliplatin/Mapa/hyperthermia treatment. Phosphorylation-Bcl-xL was stained with anti-p-Bcl-xL antibody. HA-Bcl-xL-WT, HA-Bcl-xL-S62A and HA-Bcl-xL-S62D were stained with anti-HA antibody. Nucleolin, which is the major nucleolar protein, was stained with anti-nucleolin antibody. Cellular DNA was

stained with DRAQ5. Localization of p-Bcl-xL and HA were examined by confocal microscope. Combination means the treatment with oxaliplatin/Mapa/hyperthermia.

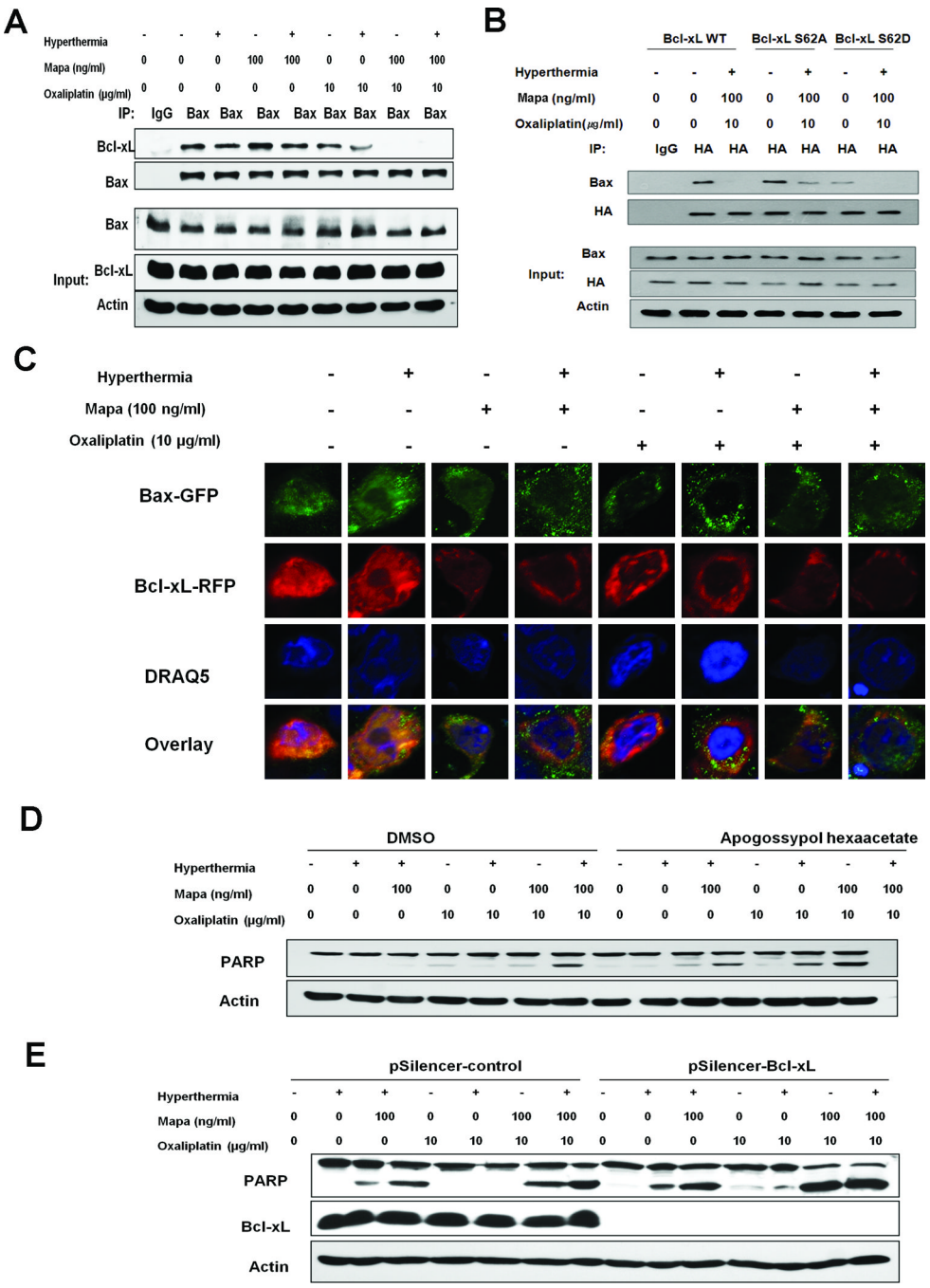

Figure 5. Role of Bcl-xL in apoptosis: The dissociation of Bcl-xL from Bax in oxaliplatin/Mapa/hyperthermia treated CX-1 cells

(**A**) Cells were treated and cell lysates were immunoprecipitated with anti-Bax antibody or mock antibody (IgG) and immunoblotted with anti-Bcl-xL or anti-Bax antibody (upper panels). The presence of Bcl-xL and Bax in the lysates was verified by immunoblotting (lower panels). (**B**) Transfectants with Bcl-xL-WT, BclxL- S62A, or Bcl-xL S62D were treated with oxaliplatin/Mapa/hyperthermia and were immunoprecipitated with anti-HA antibody or IgG and immunoblotted with anti-Bax or anti-HA antibody (upper panels). The presence of HA, Bax and actin in the lysates was examined (lower panels). (**C**) Cells were cotransfected with pBax-GFP and pBcl-xL-RFP plasmid, and 24 h later treated with

oxaliplatin/Mapa/hyperthermia. Cellular DNA was stained with DRAQ5. Localization of Bax-GFP and Bcl-xL-RFP was examined by confocal microscope. (**D**) Cells were pretreated with apogossypol hexaacetate followed by oxaliplatin/Mapa/hyperthermia. PARP cleavage was detected. (**E**) Transfectants with pSilencer-control or pSilencer-Bcl-xL were treated with oxaliplatin/Mapa/hyperthermia and immunoblotted with anti-PARP or anti-Bcl-xL antibody. Actin was shown as an internal standard.

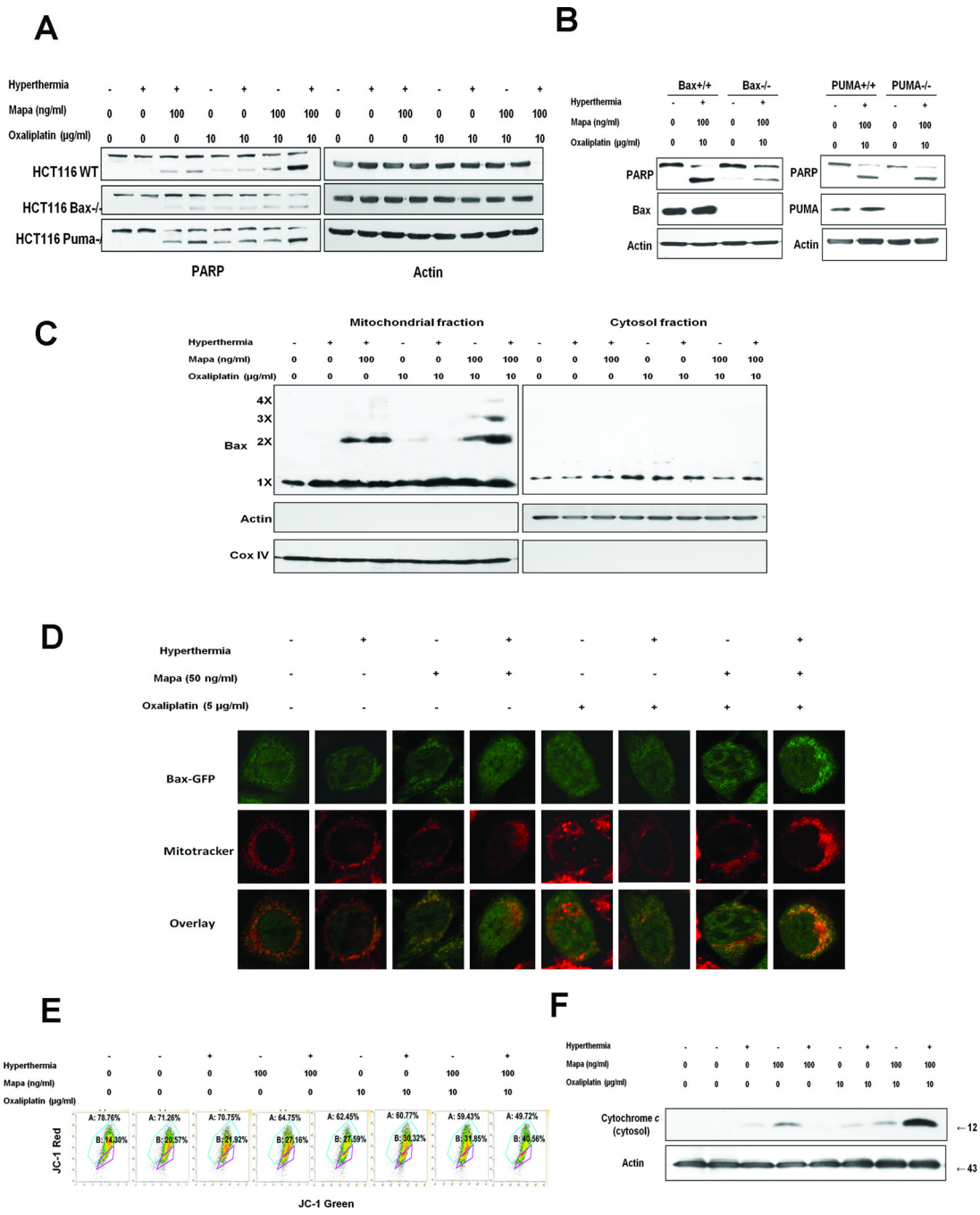

Figure 6. Bax oligomerization, localization to the mitochondria and subsequent cytochrome *c* release in Mapa/oxaliplatin/hyperthermia

(**A**) Human colon carcinoma parental HCT116 (HCT116 WT), Bax knockout HCT116 $Bax^{-/-}$and PUMA knockout HCT116 $PUMA^{-/-}$ cells were treated with oxaliplatin/Mapa/hyperthermia and immunoblotted with anti-PARP antibody. **B** HCT116 $Bax^{+/+}$HCT116 $Bax^{-/-}$HCT116 $PUMA^{+/+}$ and HCT116 $PUMA^{-/-}$ cells were treated with oxaliplatin/Mapa/hyperthermia and immunoblotted with anti-PARP, anti-Bax, or anti-PUMA antibody. (**C**) CX-1 cells were treated with oxaliplatin/Mapa/hyperthermia. Mitochondrial and cytosolic fractions were isolated and were cross-linked with dithiobis and subjected to immunoblotting with anti-Bax antibody. Bax monomer (1X) and multimers (2X, 3X, and

4X) are indicated. Actin was used as a cytosolic marker and COX IV as a mitochondrial marker. (**D**) CX-1 cells were transfected with pBax-GFP plasmid. After 24 h incubation, cells were treated with oxaliplatin/Mapa/hyperthermia. Mitochondria were stained red with MitoTracker. Localization of Bax-GFP was examined by confocal microscope. (**E**) CX-1 cells were treated with oxaliplatin/Mapa/hyperthermia and stained with JC-1 and analyzed by flow cytometry. (**F**) CX-1 cells were treated with oxaliplatin/Mapa/hyperthermia. Cytochrome c release into cytosol was determined by immunoblotting for cytochrome *c* in the cytosolic fraction. Actin was used to confirm the equal amount of proteins loaded.

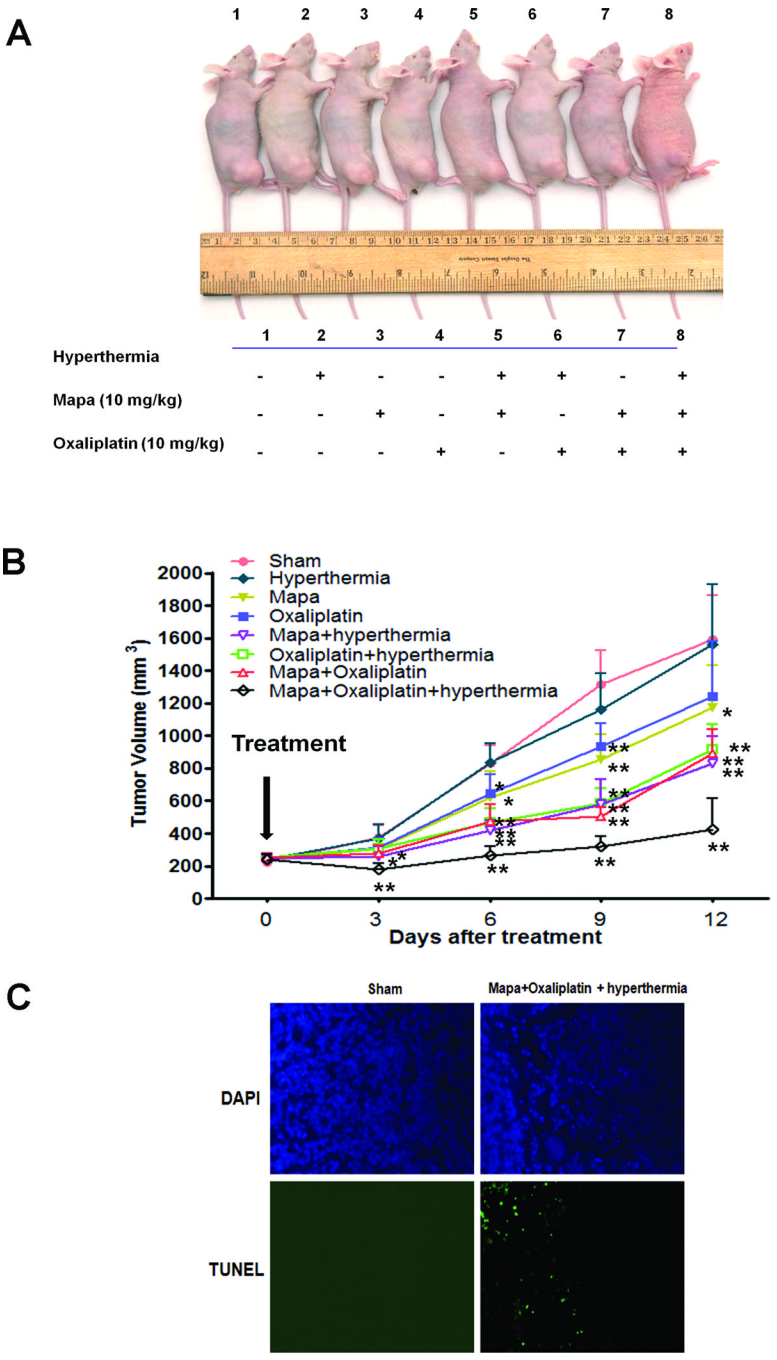

Figure 7. Effect of oxaliplatin, hyperthermia and Mapa on the growth of CX-1 xenograft tumors

NU/NU mice were inoculated subcutaneously with 1×10^6 tumor cells/mouse and the tumors were allowed to grow to 200 mm^3. 10 mg/kg oxaliplatin was administered by intraperitoneal injection and 10 mg/kg Mapa was treated by intratumoral injection and tumors were immersed in a water bath at 42°C for 1 h. (**A**) Photograph of representative tumor bearing mouse from each group 12 days after treatment. (**B**) Tumor growth curve. Error bars represent standard error of the mean from five mice. * or ** represents a statistically significant difference compared with the control group at $P<0.05$ or $P<0.01$, respectively.

(**C**) Tumor tissues were harvested at day 12 after treatment and subjected to TUNEL assay to detect apoptosis. Cell nuclei were stained with DAPI. Representative images were shown.